Magnetically induced suppression and enhancement of optical excitation of ruby at anticrossing points

Roman Kolesov
Department of Physics and Institute for Quantum Studies, Texas A&M University, College Station, Texas 77843-4242, USA
(Received 20 January 2006; published 19 April 2006)

Sharp resonances in optical excitation of ruby by laser pulses are observed as Zeeman sublevels anticross in an external magnetic field. For the R_1 optical line of ruby (694.3 nm) excitation drops when the external magnetic field strength approaches 4.14 kG while for the R_2 line (692.9 nm) it increases in 4.14 and 2.07 kG fields. A simple theoretical description of the observed effects on the basis of level mixing explains both situations.

DOI: 10.1103/PhysRevA.73.043808 PACS number(s): 42.50.Gy, 71.70.Ej, 42.50.Md

I. INTRODUCTION

Quantum interference effects are currently being studied very extensively because of the very broad spectrum of their existing and potential applications. Among them are electromagnetically induced transparency (EIT) for resonant enhancement of nonlinear interactions with reduced absorption [1], precision magnetometry [2], lasing without inversion in "hard" spectral regions [3], etc. Most experimental works are being done in alkali-metal vapors, mostly rubidium and cesium. Though rubidium vapor is an excellent medium for studying new physics of quantum interference phenomena, investigation and implementation of the latter in room-temperature solids is required for their successful application in real devices.

So far, most experimental works related to studying quantum interference phenomena in solids were performed at cryogenic temperatures [4,5]. The requirement for low temperature of the sample comes from the fact that in most solids dephasing processes are very fast due to efficient interaction of electrons with phonons. However, coherent population trapping (CPT), the most fundamental quantum interference optical phenomenon, has been demonstrated recently in room-temperature ruby [6]. The most important physical property of ruby, which allowed observation of CPT at room temperature, is the absence of resonant inelastic phonon scattering between ground-state Zeeman sublevels (so called Orbach relaxation). In the work mentioned above, it was stated that similar effects can be observed in many optical crystals doped with such ions as Cr^{3+}, Eu^{2+}, Gd^{3+}, and several others. All of them experience very slow Orbach relaxation when incorporated in solids.

In the present paper, I report experimental results and their qualitative theoretical explanation on how optical quantum interference phenomena can be induced in a room-temperature solid medium by a static magnetic field. Typically, these phenomena occur in multilevel optical media under the conditions when two or more paths of optical absorption interfere. This happens when different energy levels of the atomic system are mixed by some external driving electromagnetic field whose frequency is resonant with the atomic transition being driven. For example, microwave-induced transparency in ruby was demonstrated in [5] by driving the Zeeman transition with 16.3 GHz radiation. However, if two electronic levels have equal energies, the transition between them can be efficiently driven by a dc magnetic or electric field. In the particular case of ruby, this situation can be realized when Zeeman sublevels of the ground state are anticrossed in the external magnetic field.

It is worth mentioning that interference phenomena based on atomic coherence at level anticrossing points have been studied by different authors in several solid-state compounds. One of the most interesting effects induced by level anticrossing was observation of EIT at nuclear Mössbauer transitions of ^{57}Fe in $FeCO_3$ [7]. As for ruby, the effects of level anticrossing were studied by van der Ziel and Bloembergen [8] and by Fukuda *et al.* [9]. In these works the authors studied the behavior of optically induced magnetization. The magnetization originates either from selective depletion of ground-state Zeeman sublevels or from excitation of electronic coherence between them. All these experiments were done at room temperature and can be viewed as precursors of the present investigation. However, no effect on the optical response of ruby was reported. Rather recently, a proposal for observation of EIT near a level anticrossing of the Cr^{3+} ion in ruby was made in [10]. However, this theoretical proposal was based on the assumption of cryogenic temperature of the ruby sample. In the present paper, it is experimentally demonstrated that level mixing at the anticrossing point leads to changes in the efficiency of optical excitation of Cr^{3+} ions and, therefore, to magnetically induced transmission or absorption.

The paper is organized in the following way. In the next section, the structure of Cr^{3+} electronic levels and optical properties of ruby are reviewed. In Sec. III, the experimental arrangement is described and the experimental results are presented. A theoretical explanation of these results is presented in Sec. IV. It includes evaluation of optical selection rules near level anticrossing points and examination of a simplified three-level model of the atomic medium showing how modified selection rules can affect optical excitation efficiency under the condition of level mixing. The main results of the present work are summarized in Sec. V.

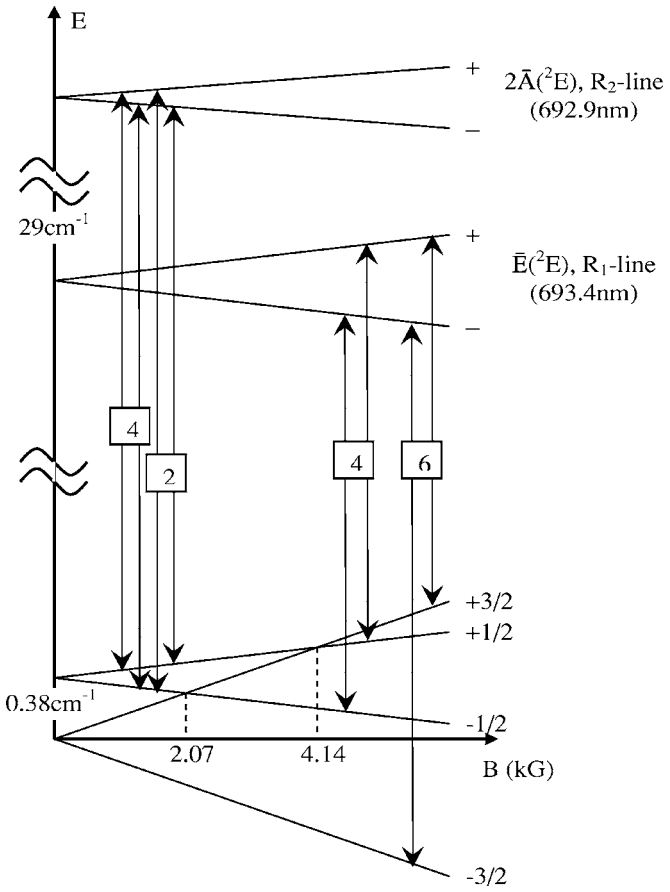

FIG. 1. Energy levels of Cr^{3+} ion in ruby vs the magnetic field along the c axis. Allowed optical transitions between different Zeeman sublevels of the ground state and of the two excited optical states for linear σ polarization are indicated by arrows. Relative oscillator strengths are given in boxes.

II. LEVEL STRUCTURE AND OPTICAL SELECTION RULES OF Cr^{3+} ION IN RUBY

Ruby ($Al_2O_3:Cr^{3+}$) is one of the most studied crystals from the viewpoint of the optical and magnetic properties of the dopant Cr^{3+} ion. The structure of the electronic energy levels of Cr^{3+} in ruby is shown in Fig. 1. The spin-3/2 ground state consists of two Kramers doublets separated by 0.38 cm^{-1} (11.47 GHz) with the $\pm 1/2$ doublet lying above the $\pm 3/2$ one. The spin Hamiltonian describing Zeeman energy levels in the external magnetic field reads as follows:

$$H_{gs} = \mu_B(g_{||}B_{||}S_z + g_{\perp}\mathbf{B}_{\perp}\cdot\mathbf{S}_{\perp}) + D\left(S_z^2 - \frac{S(S+1)}{3}\right). \quad (1)$$

Here the quantization axis is chosen along the crystal axis, μ_B is the Bohr magneton, $g_{||}=1.982$ and $g_{\perp}=1.987$ are the ground-state g factors in the directions parallel and perpendicular to the crystal axis respectively, $2D=-11.47$ GHz is the ground-state zero-field splitting, and $B_{||}$ and $\mathbf{B}_{\perp}$ are the longitudinal and transverse magnetic field components, respectively. With the magnetic field being exactly parallel to the crystal axis, $S_z=\pm 1/2, \pm 3/2$ remain good quantum numbers independent on the magnetic field strength. The states

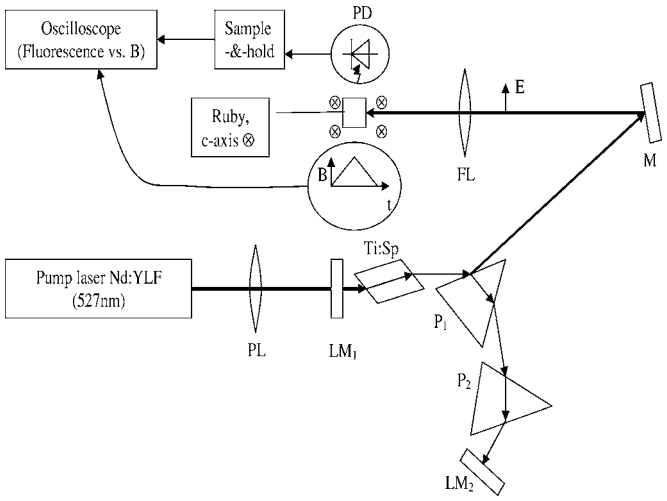

FIG. 2. Schematics of the experimental setup. Most abbreviations are self-explaining. The polarization of laser light is in the horizontal plane as indicated on the figure. The dispersion prism P_1 serves also as an output coupler for the Ti:sapphire laser. The laser is tuned with the LM_2 mirror. The fluorescence is detected by a photodiode PD and measured 1 ms after the pulse as a function of the external magnetic field.

$|-1/2\rangle$ and $|+3/2\rangle$ cross (become of the same energy) at 2.07 kG while the states $|+1/2\rangle$ and $|+3/2\rangle$ cross at 4.14 kG. However, if there is slight misalignment between the directions of the magnetic field and the crystal axis, the above pairs of states strongly mix near the crossing points, i.e., the energy levels become linear combinations of pure spinstates. The population relaxation between Zeeman sublevels is known to be in the microsecond range [11].

There are two excited optical states giving rise to two strong absorption and emission lines of ruby known as R_1 (694.3 nm) and R_2 (692.9 nm) lines. Both states are Kramers doublets. The full width at half maximum of both lines at room temperature is 11 cm^{-1} (330 GHz) with the separation between the levels being 29 cm^{-1}. Both optical transitions are broadened homogeneously. The population decay from the two excited optical levels is very slow (3 ms) while the population exchange between them is very fast at room temperature (of the order of picoseconds). Thus, the four Zeeman sublevels of the excited states are always equally populated at room temperature.

Let us consider polarization selection rules for the case when the incident light has linear σ polarization (the **E** vector of the optical wave is perpendicular to the c axis). The oscillator strengths of the transitions between different pairs of ground-state and excited-state Zeeman sublevels have been calculated by Tanabe and Sugano [12]. For 692.9 nm transition only $|\pm 1/2\rangle$ levels are involved in interaction with resonant radiation. Thus, an admixture of $|\pm 1/2\rangle$ states to the noninteracting $|+3/2\rangle$ one at anticrossing points has to lead to change in the absorptive properties of ruby. In the case of the R_1 line, all four ground-state sublevels interact with optical radiation. However, as will be shown below, at a level anticrossing point one of the coherent superpositions of Zeeman states becomes noninteracting with optical radiation. This effect can also be seen in the optical absorption of ruby.

The experimental details and results are given in the next section while a qualitative theoretical explanation of the obtained experimental results is presented in Sec. IV.

III. EXPERIMENTAL PROCEDURE AND RESULTS

A ruby crystal of dimensions $5\times5\times3$ mm^3 with the c axis being perpendicular to the 5×5 mm^2 faces and chromium concentration 0.002 wt % was obtained from Scientific Materials Corp. It was placed into a homemade electromagnet able to produce magnetic fields up to $\approx$6 kG. The crystal axis was oriented along the magnetic field. It was illuminated with a homemade linearly polarized pulsed Ti:sapphire laser capable of delivering $\approx$1 mJ at wavelengths corresponding to either the R_1 or R_2 ruby line. The pulse repetition rate was 82.4 Hz to ensure that the time interval between the two subsequent pulses ($\approx$12 ms) was several times longer than the excited-state population decay rate ($T_1=3$ ms for room-temperature ruby). This ensures that before each laser pulse all chromium ions are in the ground state. The laser polarization was perpendicular to the crystal axis. The laser output was focused onto the crystal with a 10 cm focal length lens so that the beam size at the sample was $\sim$100 μm. The laser linewidth was narrower than the widths of the $R_{1,2}$ absorption lines though the laser was multimode. The pulse duration was $\approx$34 ns. Laser-induced fluorescence was collected through one of the 3×5 mm^2 faces onto a photodiode. 1 ms after the pulse, the photodiode signal was measured and stored in a sample-and-hold aquisition system until the arrival of the next pulse. The aquisition system reading was then plotted as a function of the external magnetic field. The latter was slowly periodically scanned in the vicinity of the two anticrossings of the ruby ground-state Zeeman sublevels: the 4.14 kG anticrossing of the $|+1/2\rangle$ and $|+3/2\rangle$ states and the 2.07 kG anticrossing of the $|-1/2\rangle$ and $|+3/2\rangle$ states. The scan rate was 0.16 Hz (6 s period). The schematics of the experimental setup is shown in Fig. 2.

The plots of laser-induced fluorescence as a function of the magnetic field are presented in Figs. 3 and 4. In the vicinity of the 4.14 kG anticrossing the ruby fluorescence drops if excited by 694.3 nm (R_1-line) radiation and grows under 692.9 nm (R_2-line) excitation (see Fig. 3). In each case the change in the fluorescence intensity is about 4–5%. Each resonance has Lorentzian shape with the half width at half maximum (HWHM) being $\approx$60 G. As for the other anticrossing at 2.07 kG, the magnetic field dependence of the fluorescence under R_2-line excitation indicates a sharp but weak increase ($\approx$0.6% in amplitude and $\approx$10 G HWHM). No noticeable dependence of the laser-induced fluorescence on the magnetic field near the 2.07 kG anticrossing is detected under R_1-line excitation.

In the following section, a theoretical interpretation of the observed effects will be given.

IV. THEORETICAL CONSIDERATION AND DISCUSSION

A. Equation describing Cr^{3+} eigenstates and eigenenergies

In general, each ground-state Zeeman sublevel can be described as a superposition of bare spin states $|\pm1/2,\pm3/2\rangle$ as follows:

$$\Psi=\sum_{i=\pm1/2,\pm3/2} c_i|S_z=i\rangle. \tag{2}$$

We choose the coordinate system in such a way that its x axis is along the transverse component of the magnetic field. We also neglect the slight difference between the two g factors: $g_\parallel=g_\perp=g$. The Hamiltonian (1) yields the following matrix equation for the coefficients c_i:

$$\begin{pmatrix} -1-\frac{3}{2}m\cos\alpha-e^{(k)} & \frac{\sqrt{3}}{2}m\sin\alpha & 0 & 0 \\ \frac{\sqrt{3}}{2}m\sin\alpha & 1-\frac{1}{2}m\cos\alpha-e^{(k)} & m\sin\alpha & 0 \\ 0 & m\sin\alpha & 1+\frac{1}{2}m\cos\alpha-e^{(k)} & \frac{\sqrt{3}}{2}m\sin\alpha \\ 0 & 0 & \frac{\sqrt{3}}{2}m\sin\alpha & -1+\frac{3}{2}m\cos\alpha-e^{(k)} \end{pmatrix} \begin{pmatrix} c^{(k)}_{-3/2} \\ c^{(k)}_{-1/2} \\ c^{(k)}_{+1/2} \\ c^{(k)}_{+3/2} \end{pmatrix}=0. \tag{3}$$

Here α is the angle between the magnetic field and the c axis, $m=g\mu_B B/|D|$, k enumerates eigenstates and eigenenergies, and $e^{(k)}$ is the energy of the kth state normalized by $|D|$. In addition, the center of mass of the four states in zero magnetic field is set to 0.

B. Eigenstates and energies at 4.14 kG anticrossing

Near the 4.14 kG anticrossing the Zeeman sublevels $|+1/2\rangle$ and $|+3/2\rangle$ are coupled directly by the transverse magnetic field since the transition between these states is magnetically allowed. Therefore, the above matrix equation (3) can be reduced to the following:

$$\begin{pmatrix} 1+\frac{1}{2}m\cos\alpha - e^{(\pm)} & \frac{\sqrt{3}}{2}m\sin\alpha \\ \frac{\sqrt{3}}{2}m\sin\alpha & -1+\frac{3}{2}m\cos\alpha - e^{(\pm)} \end{pmatrix} \begin{pmatrix} c_{+1/2}^{(\pm)} \\ c_{+3/2}^{(\pm)} \end{pmatrix} = 0. \quad (4)$$

Here the index (±) represents the two resulting eigenstates. The eigenvalues of the 2×2 interaction matrix can be represented in the following way:

$$e^{(\pm)} = m\cos\alpha \pm \frac{\sqrt{3-2\cos^2\alpha}}{2}\sqrt{\left(m-\frac{2\cos\alpha}{3-2\cos^2\alpha}\right)^2 + 12\left(\frac{\sin\alpha}{3-2\cos^2\alpha}\right)^2}. \quad (5)$$

This expression gives the minimum distance between the anticrossing levels and the magnitude of the magnetic field at which this distance is achieved:

$$\Delta e_{min} = \sqrt{\frac{12\sin^2\alpha}{3-2\cos^2\alpha}}, \quad m_{min} = \frac{2\cos\alpha}{3-2\cos^2\alpha}. \quad (6)$$

It is convenient to introduce $\Delta m = m - m_{min}$. Assuming $\alpha \ll 1$, the energies and the mixing coefficients of the two levels can be written in the following form:

$$e^{(\pm)} = 2 + \Delta m \pm \tfrac{1}{2}\sqrt{\Delta m^2 + 12\alpha^2}, \quad \Delta e_{min} = \sqrt{12\alpha^2}, \quad (7)$$

$$(c_{+1/2}^{(\pm)})^2 = \frac{6\alpha^2}{\Delta m^2 + 12\alpha^2 \pm \Delta m\sqrt{\Delta m^2 + 12\alpha^2}}, \quad (8)$$

$$(c_{+3/2}^{(\pm)})^2 = 1 - (c_{+1/2}^{(\pm)})^2.$$

Maximum mixing occurs at $\Delta m = 0$ with the squares of both coefficients being 1/2.

C. Effect of level mixing on the optical absorption at 4.14 kG

In order to understand how level mixing can affect the optical absorption of a resonant laser pulse, let us consider a simple three-level model shown in Fig. 5. Levels 1 and 2 represent two Zeeman sublevels of the Cr^{3+} ion. They are coupled to the same level 3 by the same optical field, but the oscillator strengths of the two transitions are different. All population relaxation processes are neglected at the time scale of the laser pulse action. We also neglect the optical excitation of Zeeman coherence which can lead to coherent population trapping [6]. This fact will be verified later. Under these assumptions, the system can be described by simple balance equations:

$$\dot{n}_1 = P_1(n_3 - n_1), \quad (9)$$

$$\dot{n}_2 = P_2(n_3 - n_2), \quad (10)$$

$$\sum_{i=1}^{3} n_i = 1, \quad (11)$$

where n_i is the population of the ith level, and P_i is the optical pumping rate at the corresponding transition. The initial populations are $n_3(0)=0$ and $n_1(0)=n_2(0)=1/2$. For simplicity, we assume a square shape of the laser pulse so that P_i=const during the pulse action. The solution of the above set of equations yields the following expression for n_3:

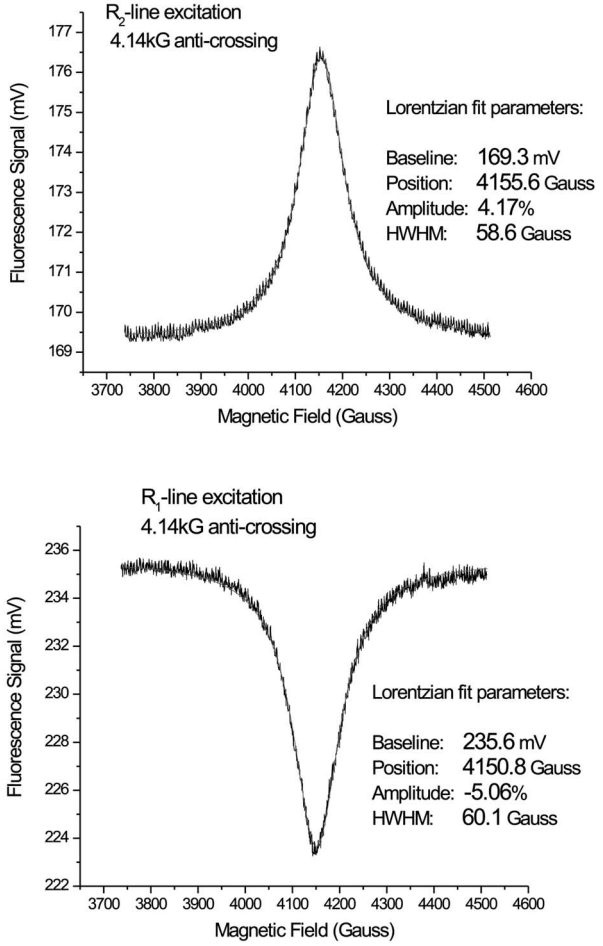

FIG. 3. Laser-induced fluorescence as a function of the magnetic field at 4.14 kG anticrossing. The parameters of the Lorentzian fit are included in the graphs.

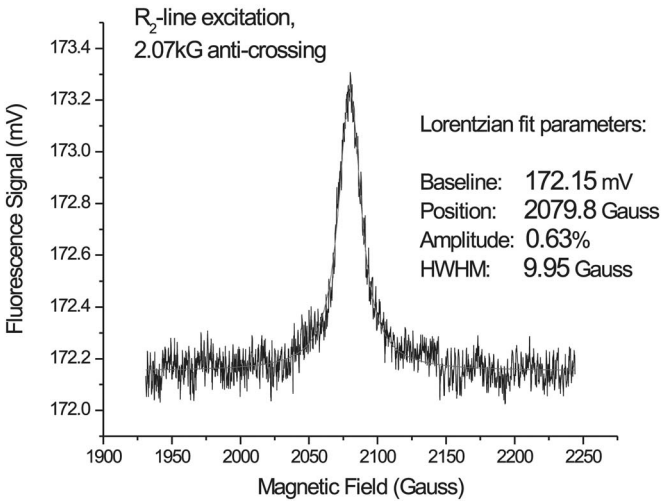

FIG. 4. Dependence of the fluorescence on the magnetic field near 2.07 kG anticrossing under R_2-line excitation.

$$n_3 = \frac{1}{3} + \frac{P_1 + P_2 - 2P_{12}}{12P_{12}} e^{-(P_1+P_2-P_{12})t} - \frac{P_1 + P_2 + 2P_{12}}{12P_{12}} e^{-(P_1+P_2+P_{12})t}, \quad (12)$$

where $P_{12}=\sqrt{P_1^2-P_1P_2+P_2^2}$. It is clear that at $t\to\infty$ the pumping field tends to equalize the populations of all three levels since no population relaxation processes are present in the system. However, the time at which this equilibrium is reached is determined by the longest time scale $\tau=(P_1+P_2-P_{12})^{-1}$. For optical pulses shorter than this characteristic time the resulting population of level 3 strongly depends on the ratio of the pumping rates P_1/P_2 even if the total pumping rate $P=P_1+P_2$ is the same. Let us consider the two extreme cases (1) $P_1=P_2=P/2$ and (2) $P_1=P$, $P_2=0$. In the first case, $n_3=(1-e^{-3Pt/2})/3$ exponentially approaches 1/3. In the second one, $n_3=(1-e^{-2Pt})/4$ approaches 1/4 since $\tau=\infty$. In other words, the optical field tends to equalize the populations of levels 1 and 3 without affecting n_2. Thus, the difference in excitation efficiency in those two cases can lead to as high as 1/12 difference in the excited-state population, i.e., 25% decrease or 33% increase.

How does this apply to the 4.14 kG anticrossing in ruby? In the case of the R_2-line excitation, away from the anticrossing point only the transitions $|+1/2\rangle \leftrightarrow |\pm 2\bar{A}\rangle$ interact with the optical pumping field, but not $|+3/2\rangle \leftrightarrow |\pm 2\bar{A}\rangle$. However, as states mix, both levels

$$|\pm A_4\rangle = c_{+1/2}^{(\pm)}|+1/2\rangle + c_{+3/2}^{(\pm)}|+3/2\rangle \quad (13)$$

give their contributions to pumping of the excited states. This explains the experimentally observed enhancement in excitation efficiency. The maximum achievable contrast can be easily estimated as follows. Away from the anticrossing point, optical pumping tends to equalize the populations of six states: the $|\pm 1/2\rangle$ ground-state sublevel and four Zeeman sublevels of the excited state. At the same time, the total population in these six states is 1/2 because the other 1/2 is

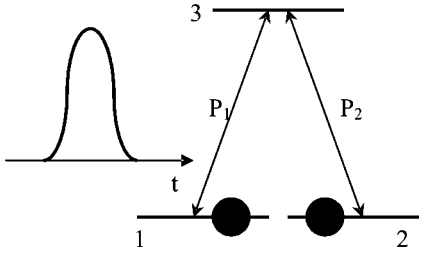

FIG. 5. Three-level model illustrating pumping near anticrossings in ruby.

stored in $|\pm 3/2\rangle$ states. Thus, the maximum population in the excited states is $4/6\times 1/2=1/3$. At the anticrossing point, the optical field tends to equalize the populations of seven states: $|\pm A_4\rangle$, $|-1/2\rangle$, and four excited-state sublevels. The total population of these seven states is 3/4 (1/4 is stored in $|-3/2\rangle$) resulting in maximum optical excitation $4/7\times 3/4=3/7$. Thus, at the anticrossing point the excited-state population can theoretically increase by 2/21 and the corresponding increase in the fluorescence intensity can be as high as $(2/21)/(1/3)\approx 28.6\%$. This number gives the maximum achievable contrast of increased excitation efficiency at the anticrossing point. In real experiment, this value was significantly lower($\sim 5\%$) indicating that the pulse energy flux was lower than the one required for saturation of the optical transition, i.e., $PT<1$ with T being the pulse duration. However, further increase in laser pulse energy was not attempted because of the risk of crystal breakdown. Additional factors reducing the magnitude of the excitation enhancement might be background fluorescence from the laser beam wings and, possibly, the fact that the beam focal waist is shorter than the crystal length.

In the case of rather small pumping energy flux $PT<1$, the width of the resonance is determined by the angle between the c axis and the magnetic field. It is convenient to introduce the mixing degree x so that $P_1=xP$ and $P_2=(1-x)P$. The relative increase of excitation efficiency is given by $r(x)=[n_3(x)-n_3(x=0)]/n_3(x=0)$. Series expansion of $r(x)$ to the first order in PT gives one $r(x)=PTx(1-x)$. At $x=1/2$, $r=PT/4$. The excitation efficiency enhancement drops to $PT/8$ (half of its maximum value) at $x=(2\pm\sqrt{2})/4$. Since $x=(c_{+1/2}^{(+)})^2$ and $1-x=(c_{+1/2}^{(-)})^2$, it is easy to find the magnitude of the magnetic field corresponding to the half-width of the resonance:

$$|\Delta m| = 2\sqrt{3}\alpha. \quad (14)$$

The experimental width of the 4.14 kG resonance ($\Delta B\approx 60$ G HWHM) yields $\alpha=0.48^\circ$. This angle gives the minimum frequency separation between the $|\pm A_4\rangle$ states $2\sqrt{3}\alpha$ or 166 MHz. This value is much greater than the spectral width of the laser pulse intensity (laser pulse duration ≈ 34 ns). Thus, optical excitation of Zeeman coherence between levels $|\pm A_4\rangle$ and, consequently, coherent population trapping [6] can be neglected.

Excitation at the R_1 ruby line represents exactly the opposite situation. Away from the 4.14 kG anticrossing point the intensity ratio $P_1/P=1-P_2/P=0.4$ since the optical transi-

tions $|+1/2\rangle \leftrightarrow |+\bar{E}\rangle$ and $|+3/2\rangle \leftrightarrow |+\bar{E}\rangle$ have relative oscillator strengths 4 and 6, respectively (see Fig. 1). However, near the anticrossing point the optical transitions $|\pm A_4\rangle \leftrightarrow |+\bar{E}\rangle$ have relative oscillator strengths $[2\sqrt{x}+\sqrt{6(1-x)}]^2$ and $(2\sqrt{1-x}-\sqrt{6x})^2$, respectively. The latter vanishes at $x=0.4$. Thus, as the states $|+1/2\rangle$ and $|+3/2\rangle$ mix, one should expect reduction of excitation efficiency. This explains the drop in the fluorescence intensity under R_1-line excitation.

D. Eigenstates of Cr^{3+} ion and effect of level mixing on optical excitation at 2.07 kG anticrossing point

The levels $|-1/2\rangle$ and $|+3/2\rangle$ cross at 2.07 kG. The transition between them is magnetic-dipole forbidden; thus, they can mix only via magnetic perturbation of second order in the transverse magnetic field. This perturbation acts through level $|+1/2\rangle$. The matrix equation describing the eigenstates reads as follows:

$$\begin{pmatrix} 1-\frac{1}{2}m\cos\alpha-e^{(k)} & m\sin\alpha & 0 \\ m\sin\alpha & 1+\frac{1}{2}m\cos\alpha-e^{(k)} & \frac{\sqrt{3}}{2}m\sin\alpha \\ 0 & \frac{\sqrt{3}}{2}m\sin\alpha & -1+\frac{3}{2}m\cos\alpha-e^{(k)} \end{pmatrix} \begin{pmatrix} c_{-1/2}^{(k)} \\ c_{+1/2}^{(k)} \\ c_{+3/2}^{(k)} \end{pmatrix} = 0. \tag{15}$$

Since we are interested in the region close to the anticrossing point, one can eliminate $c_{+1/2}^{(k)}$ by solving the second equation of the above set with $m \approx 1$, $\alpha \ll 1$, and $e^{(k)} \approx 1/2$:

$$c_{+1/2}^{(k)} = -\alpha\left(c_{-1/2}^{(k)} + \frac{\sqrt{3}}{2}c_{+3/2}^{(k)}\right). \tag{16}$$

Thus, in the vicinity of the anticrossing point the matrix equation for $c_{-1/2}^{(\pm)}$ and $c_{+3/2}^{(\pm)}$ takes the following form:

$$\begin{pmatrix} \frac{1}{2}-\frac{\Delta m}{2}-\frac{3}{4}\alpha^2-e^{(\pm)} & -\frac{\sqrt{3}}{2}\alpha^2 \\ -\frac{\sqrt{3}}{2}\alpha^2 & \frac{1}{2}+\frac{3\Delta m}{2}-\frac{3}{2}\alpha^2-e^{(\pm)} \end{pmatrix} \begin{pmatrix} c_{-1/2}^{(\pm)} \\ c_{+3/2}^{(\pm)} \end{pmatrix} = 0, \tag{17}$$

where $\Delta m = m-1$. The eigenenergies of the above equation are given by the following expression:

$$e^{(\pm)} = \frac{1}{8}\left[4+4\left(\Delta m-\frac{3}{8}\alpha^2\right) - \frac{15}{2}\alpha^2 \pm \sqrt{64\left(\Delta m-\frac{3}{8}\alpha^2\right)^2+48\alpha^4}\right]. \tag{18}$$

The minimum energy separation occurs at $\Delta m_0 = 3\alpha^2/8$. The corresponding eigenstates are given by the formulas

$$|+A_2\rangle = \sqrt{x}|-1/2\rangle + \sqrt{1-x}|+3/2\rangle, \tag{19}$$

$$|-A_2\rangle = \sqrt{1-x}|-1/2\rangle - \sqrt{x}|+3/2\rangle, \tag{20}$$

where

$$x = 1-\frac{48\alpha^4}{48\alpha^4+[8(\Delta m-\Delta m_0)+\sqrt{64(\Delta m-\Delta m_0)^2+48\alpha^4}]^2}. \tag{21}$$

The situation with the R_2-line excitation resembles the one at the 4.14 kG anticrossing. However, there are two significant complications. First of all, the minimum frequency distance between the two eigenstates is $\Delta e_{min} = \sqrt{3}\alpha^2$ or ≈ 0.7 MHz in the frequency domain. Under this condition the effect of coherent population trapping cannot be neglected since the two optical transitions originating at the $|\pm A_2\rangle$ levels form a Λ system and the frequency separation between those levels is smaller than the inverse pulse duration T^{-1}. At the same time, the characteristic width of the anticrossing should be of the same order, i.e., of the order of a few megahertz. However, it is well known that Zeeman transitions of Cr^{3+} are inhomogeneously broadened with characteristic width ~ 10 G (tens of megahertz) [13]. This means that at each particular magnetic field at the anticrossing point level mixing occurs only for a portion of all atoms. The observed width of the 2.07 kG resonance (see Fig. 4) agrees well with the ~ 10 G inhomogeneous broadening mentioned above. Both effects of CPT and inhomogeneous broadening account for a significant drop in amplitude of the R_2-excitation enhancement at 2.07 kG as compared to the 4.14 kG case. The effect of inhomogeneous broadening is not significant at the 4.14 kG anticrossing since its intrinsic width was greater than the inhomogeneous one.

In order to check the fact that excitation enhancements at 2.07 and at 4.14 kG have the same origin, the crystal was tilted so that the c axis made an angle of $\approx 5^\circ$ with the magnetic field direction. Under these circumstances, the amplitude of the resonance at the 2.07 kG anticrossing became the same as the one at 4.14 kG (see Fig. 6) for the reason that the intrinsic width of the 2.07 kG anticrossing (this width is pro-

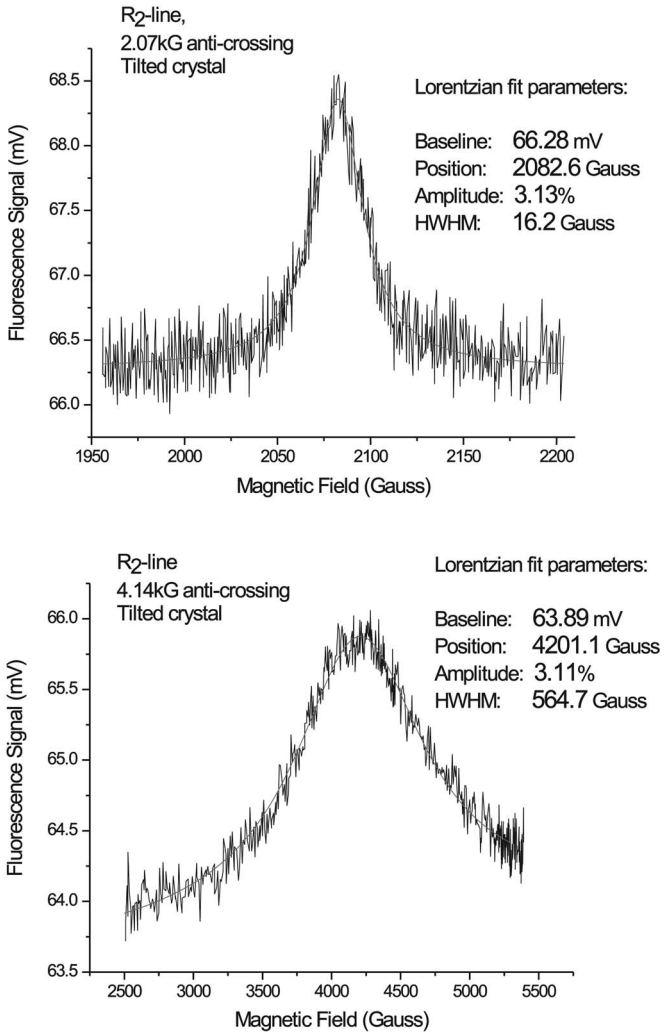

FIG. 6. Fluorescence as a function of the magnetic field near the two anticrossings under R_2-line excitation when the crystal is tilted at $\approx 5^\circ$. In both cases the excitation enhancement is $\approx 3\%$.

portional to α^2) became larger than the inhomogeneous broadening. At the same time, the minimum distance between the anticrossed levels became greater than the pulse intensity spectral width, and thus CPT did not play any role either.

Finally, let us consider the case of R_1-line excitation near the 2.07 kG anticrossing. The situation is very much different from the one at the 4.14 kG anticrossing because $|-1/2\rangle$ and $|+3/2\rangle$ are optically coupled to different sublevels of the excited optical state ($|-\bar{E}\rangle$ and $|+\bar{E}\rangle$, respectively). Near the anticrossing point the matrix elements of the optical transitions originating at levels $|\pm A_2\rangle$ are given by the following expressions:

$$\langle +\bar{E}|\mu|+A_2\rangle \propto -\sqrt{6(1-x)}, \tag{22}$$

$$\langle +\bar{E}|\mu|-A_2\rangle \propto \sqrt{6x}, \tag{23}$$

$$\langle -\bar{E}|\mu|+A_2\rangle \propto 2\sqrt{x}, \tag{24}$$

$$\langle -\bar{E}|\mu|-A_2\rangle \propto 2\sqrt{1-x}, \tag{25}$$

where x is the degree of mixing defined above and μ is the optical dipole moment operator. The total rates at which population is pumped out of the states $|\pm A_2\rangle$ are

$$P(+A_2) \propto 6-2x, \quad P(-A_2) \propto 4+2x. \tag{26}$$

The ratio of the pumping rates changes from 4:6 to at most 5:5; thus, both levels are essentially involved in optical interaction at any degree of mixing and one cannot expect significant changes in pumping efficiency. At the same time, CPT cannot be expected for the reason that the two Λ systems $|-A_2\rangle \leftrightarrow |\pm\bar{E}\rangle \leftrightarrow |+A_2\rangle$ tend to excited Zeeman coherence between levels $|\pm A_2\rangle$ in the opposite phase. For a Λ system, Zeeman coherence excitation is proportional to the product of the optical dipole elements. For the two Λ systems mentioned above, the products of the optical dipole elements are proportional to $-6\sqrt{x(1-x)}$ and $4\sqrt{x(1-x)}$. Even though those two Λ systems do not exactly compensate each other, one cannot expect an observable effect of CPT on the fluorescence excitation efficiency. This reasoning fully agrees with the experimental results reported above.

V. CONCLUSION

The effect of Zeeman sublevel mixing at the magnetic anticrossing points on the optical excitation properties is investigated experimentally at the ruby red absorption and emission lines. Though the excitation of Zeeman coherence by optical means near level anticrossing points was studied in room-temperature ruby long ago [8,9], the back action of the excited coherence on the optical properties of the crystal was never reported to the best of my knowledge. It is shown that significant enhancement or reduction of optical excitation can be produced by abrupt changes of optical selection rules near anticrossing points. It is worth noting that the reported effects are observable only in the pulsed regime of laser operation, i.e., they have a transient nature. Though the presented theoretical treatment correctly explains the nature of both enhancement and reduction of excitation efficiency, these effects can be alternatively viewed as electromagnetically induced absorption and/or transparency in the presence of a strong driving field. The coherent driving occurs due to the transverse component of the dc magnetic field. In the case of the 4.14 kG anticrossing, the driving field directly couples $|+1/2\rangle$ and $|+3/2\rangle$ states while near the 2.07 kG point the states $|-1/2\rangle$ and $|+3/2\rangle$ are coupled by two-photon interaction via the $|+1/2\rangle$ state. In that sense, the two situations illustrate EIA and EIT in a Λ or ladder system or in a double-Λ system, respectively.

ACKNOWLEDGMENTS

The author is grateful to Yuri Rostovtsev, Elena Kuznetsova, Olga Kocharovskaya, and Marlan O. Scully for valuable discussions. The work was financially supported by NSF and AFOSR.

[1] S. E. Harris, J. E. Field, and A. Imamoglu, Phys. Rev. Lett. **64**, 1107 (1990); M. Fleischhauer, A. Imamoglu, and J. P. Marangos, Rev. Mod. Phys. **77**, 633 (2005).
[2] D. Budker, W. Gawlik, D. F. Kimball, S. M. Rochester, V. V. Yashchuk, and A. Weis, Rev. Mod. Phys. **74**, 1153 (2002).
[3] J. Mompart and R. Corbalan, J. Opt. B: Quantum Semiclassical Opt. **2**, R7 (2000).
[4] C. J. Wei and N. B. Manson, Phys. Rev. A **60**, 2540 (1999); A. V. Turukhin *et al.*, Phys. Rev. Lett. **88**, 023602 (2001); M. Phillips and H. L. Wang, *ibid.* **89**, 186401 (2002).
[5] Y. Zhao, C. Wu, B. S. Ham, M. K. Kim, and E. Awad, Phys. Rev. Lett. **79**, 641 (1997).
[6] R. Kolesov, Phys. Rev. A **72**, 051801(R) (2005).
[7] R. Coussement *et al.*, Phys. Rev. Lett. **89**, 107601 (2002).
[8] J. P. van der Ziel and N. Bloembergen, Phys. Rev. **138**, A1287 (1965).
[9] Y. Fukuda, Y. Takagi, K. Yamada, and T. Hashi, J. Phys. Soc. Jpn. **42**, 1061 (1977).
[10] R. N. Shakhmuratov, A. Szabo, G. Kozyreff, R. Coussement, J. Odeurs, and P. Mandel, Phys. Rev. A **62**, 043405 (2000).
[11] R. E. Michel, J. Phys. Chem. Solids **13**, 164 (1960).
[12] S. Sugano and Y. Tanabe, J. Phys. Soc. Jpn. **13**, 880 (1958); **13**, 899 (1958); M. O. Schweika-Kresimon, J. Gutschank, and D. Suter, Phys. Rev. A **66**, 043816 (2002).
[13] R. F. Wenzel and Y. W. Kim, Phys. Rev. **140**, A1592 (1965).